Optimal Coordination of Directional Overcurrent Relays Using a New Time–Current–Voltage Characteristic

Khaled A. Saleh, *Student Member, IEEE*, H. H. Zeineldin, *Senior Member, IEEE*, A. Al-Hinai, *Senior Member, IEEE*, and Ehab F. El-Saadany, *Senior Member, IEEE*

***Abstract*—With the integration of distributed generation (DG) to meshed distribution systems, the operating time of the protective system becomes a major concern in order to avoid nuisance DG tripping. This paper proposes a new time–current–voltage tripping characteristic for directional overcurrent relays (DOCRs) that can achieve a higher possible reduction of overall relays operating time in meshed distribution networks. The proposed tripping characteristic is described in detail. Moreover, the protection coordination problem is formulated as a constrained nonlinear programming problem to determine the optimal relay settings. The proposed characteristic is tested on the power distribution system of the IEEE 14 bus and IEEE 30 bus with inverter-based and synchronous-based DG units. The outcome of this study reveals that the new tripping characteristic for DOCRs achieves notable reduction in total relays' operating time over the conventional characteristic.**

***Index Terms*—Directional overcurrent relay (DOCR), distributed generation (DG), protection coordination, tripping characteristic.**

I. Introduction

PROTECTION coordination is a process of determining the primary protective devices responsible for clearing the fault as quickly as possible for each fault location, taking into account that in the event that any of the devices fail, each should be backed up by another protective device [1]. The introduction of distributed generation (DG) to the distribution network and the recent drive toward smart grids is expected to transform the distribution networks into a meshed structure resembling interconnected subtransmission systems [2]. The occurrence of faults on such meshed systems will cause bidirectional flow of short-circuit currents. Moreover, the presence of DG will affect the magnitudes and directions of the short-circuit currents resulting in a possible failure of the coordination between overcurrent relays [3]. Hence, protection schemes based on directional overcurrent relays (DOCRs) are proposed for such systems [4]–[7].

One of the most popular solutions proposed in the literature to solve the protection coordination problem of interconnected systems is the use of optimization methods [4]–[17]. The main objective is to achieve minimum possible tripping times by obtaining the optimal settings of each DOCR. In [9], an MINLP formulation for the protection coordination problem is proposed. Yet, in [10]–[13], the problem is linearized and formulated as a linear-programming (LP) problem. More recently, heuristic techniques, such as particle swarm optimization (PSO), genetic algorithm (GA), and evolutionary methods have been proposed to solve the complex and nonconvex DOCRs protection coordination problem [14]–[17]. Finally, in [5]–[7] and [18], the protection coordination problem is relaxed and formulated as nonlinear programing (NLP) problem.

Usually, DOCRs operate based on the conventional inverse time–current characteristic. According to [19], further reduction of overall tripping time is possible by investigating the tripping time characteristic equation. Since in today's technology OCRs/DOCRs are microprocessor based, the tripping time characteristic equation can be changed by reprogramming the relay. In [19], a new tripping characteristic equation was proposed for OCR based on the logarithmic function. The proposed logarithmic characteristic replaces the conventional inverse time–current characteristic equation of OCRs. The results indicate that the use of the new characteristic equation leads to a noticeable reduction of the tripping time with respect to the conventional characteristic for radial systems using OCR and, more specifically, with inverter-based DG [19]. In this paper, both inverter-based and synchronous-based DG units are considered. Synchronous generator-based DG units are taken into account due to the fact that their fault current contribution is much higher than inverter-based DG units and, thus, they have a much more profound effect on protection coordination [20]. On the other hand, although inverter-based DG units fault current contribution is only in the range of 1.5-2 p.u, they are more dominant than synchronous-based DG units especially with increased renewable energy integration [20].

Manuscript received July 01, 2013; revised September 26, 2013, December 18, 2013, and February 25, 2014; accepted July 17, 2014. This work was supported by the Masdar Institute of Science and Technology. Paper no. TPWRD-00745-2013.

K. A. Saleh and A. Al-Hinai are with the iEnergy and the Department of Electrical Engineering and Computer Science, Masdar Institute of Science and Technology, Abu Dhabi, United Arab Emirates (e-mail: ksaleh@masdar.ac.ae).

H. H. Zeineldin is with the Faculty of Engineering, Cairo University, Giza, Egypt and also with the iEnergy and the Department of Electrical Engineering and Computer Science, Masdar Institute of Science and Technology, Abu Dhabi, United Arab Emirates.

E. F. El-Saadany is with the Department of Electrical and Computer Engineering, University of Waterloo, Waterloo, ON N2L 3G1 Canada (e-mail: ehab@uwaterloo.ca).

Color versions of one or more of the figures in this paper are available online at http://ieeexplore.ieee.org.

Digital Object Identifier 10.1109/TPWRD.2014.2341666

This paper proposes a new nonstandard relay characteristic that depends not only on current magnitude but also on voltage magnitude for determining the relay operating time. The proposed characteristic, which will be denoted as the time–current-voltage characteristic, can be implemented in microprocessor-based DOCRs. The proposed relay characteristic should achieve minimum overall tripping time in the protection coordination problem of meshed distribution networks equipped with directly connected synchronous generator-based DG units as well as inverter-based DG units. In order to test and verify the effectiveness of the proposed approach, the power distribution system of the IEEE 14-bus and IEEE 30-bus standard test systems are modeled with the introduction of DG units at various locations. Moreover, the problem with the proposed characteristic is formulated as a constrained NLP problem to determine the optimal relay settings for each system. A comparative study is presented that highlights the advantages of the proposed nonstandard characteristic over the conventional time–current relay characteristics.

II. Proposed Relay Characteristic

Protection schemes based on DOCRs should provide protection against interphase faults as well as single-line-to-ground (SLG) faults. Thus, in this paper, it is assumed that all of the systems under study are equipped with three-phase DOCRs that are capable of providing protection against SLG, line-to-line (LL), double-line-to-ground (DLG), and three phase faults [21]. Protection schemes involving both phase and ground relays (based on zero- and negative-sequence currents), have not been considered in this paper.

Most of the conventional DOCRs used up till today utilize a time–current characteristic where the time changes inversely with current magnitude. The characteristic equation varies slightly depending on the type of DOCR used and the standard, which the relay manufacturer follows. In this study, the IEC 255-3 standard inverse characteristic is followed [22]. Since microprocessor-based DOCRs provide an opportunity to develop user-defined characteristics for the DOCR's overcurrent unit [23], [24], this paper proposes a new nonstandard characteristic for the DOCRs.

The proposed DOCR algorithm involves directional sensing and tripping time computation. Usually, DOCR determines the direction of the fault using the phase relationship of the voltage and current. DOCRs are equipped with three voltage transformers (VTs) for three-phase operation in addition to the three existing current transformers (CTs) to measure voltage and current, espectively [25]. Based on the measured quantities, the respective voltages and currents magnitudes and phases are computed. The algorithm used to determine the fault direction varies among different relay manufacturers in terms of how the angular relationships are sensed [25]. The 90° quadrature method is typically used for direction detection. This method involves comparing each current's phase angle with a polarizing quantity which is the line-to-line voltage between the other two phases shifted by an angle commonly referred to as the relay characteristic angle (RCA) for digital and numerical relays [25]–[29].

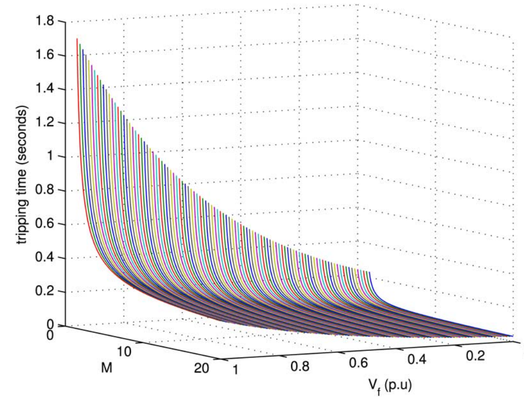

Fig. 1. Proposed relay time–current–voltage characteristic with $\mathrm{K} = 2$ and $\mathrm{TDS} = 0.1$.

Since DOCRs have VTs already installed, this paper proposes a modified DOCR characteristic for the tripping time computation that utilizes, in addition to the current, the fault voltage magnitude at the DOCR. The proposed time–current-voltage DOCR characteristic can be expressed as follows:

$$t_{ijl} = \left(\frac{1}{e^{1-V_{fijl}}}\right)^{K} \mathrm{TDS}_i \frac{A}{M_{ijl}^{B} - 1} \tag{1}$$

where t_{ijl} is the tripping time (in seconds) of relay i due to a fault type j occurrence at location l. V_{fijl} is the per-unit equivalent of the phase fault voltage magnitude measured at relay i for a fault type j at location l, while K is a constant parameter. It is worth noting that the fault voltage magnitude used in the proposed characteristic should not be used for direction comparisons. M is the multiple of pickup currents which is equal to (Isc_{ijl}/Ip_i). I_{ijl} is the short-circuit current measured at the secondary winding of the current transformer of relay i for a fault type j at location l while the pickup current Ip_i is the minimum value of current above which the relay i starts to operate. TDS_i is the time dial setting of relay i. The constants A and B are set to 0.14 and 0.02, respectively. Fig. 1 illustrates the characteristic curve for a relay with K and TDS set to 2 and 0.1, respectively.

The proposed characteristic integrates the fault voltage magnitude V_f as a third dimension to the conventional time–current characteristic which allows for additional possible conventional tripping characteristics with only three settings to set and optimize. The proposed DOCR characteristic consists of two cascaded parts. The first part is the conventional standard inverse DOCR operating characteristic equation. This part ensures maintaining the inverse time–current characteristic properties with the common relay settings (TDS and Ip). The second part of the proposed characteristic is the fault voltage magnitude exponential function with K being the third setting. An exponential function has been chosen such that the following conditions are fulfilled:

a) The proposed characteristic relies on the V_f measurement. V_f varies depending on the fault location with respect to the DOCR's location at which it is measured. This measurement can reach zero for a bolted fault occurring at the DOCR's VT terminal. Since the typical operation

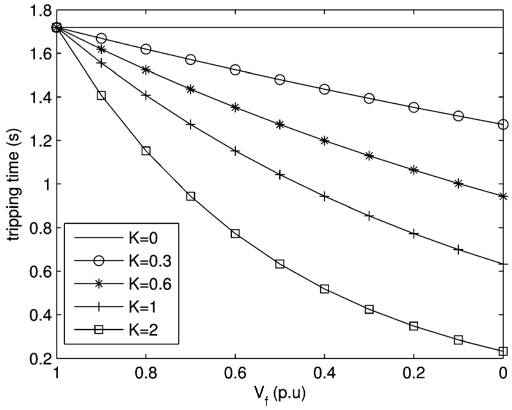

Fig. 2. Effect of the setting K on the proposed relay tripping time with $\mathrm{M} = 1.5$ and $\mathrm{TDS} = 0.1$.

time of the DOCR is about 16–20 ms [30], the exponential function is used to ensure that the operation time does not become zero when the fault voltage magnitude is zero.

b) The DOCR operating time is designed to be proportional to the drop in voltage due to the fault. A large drop in voltage signifies that the fault is closer to the relay and, thus, fast operation is needed and vice-versa. Thus, the reciprocal of the exponential is considered with the exponential superscript being $(1 - V_f)$.

c) The effect of V_f is cancelled by setting K to zero and the conventional time–current characteristic is obtained which makes the proposed approach quite flexible.

d) The exponential part has been chosen such that it does not alter the effect of TDS and Ip on the relay characteristic.

The rate of change in tripping time with respect to change in V_f is controlled by varying K (Fig. 2). Thus, in the proposed method, K is considered as an additional setting for the relay and is added to the coordination problem as an optimization variable with the intention of attaining optimal settings for each DOCR that solves the coordination problem. The parameter K can be either fixed (the same for all relays in a given system) or could be designed to have a different value for each DOCR. Both cases are considered while formulating and solving the coordination problem.

For a three-phase DOCR, three tripping times are computed that correspond to each phase, respectively. This means that the tripping time corresponding to phase A will be calculated based on phase A voltage and current magnitudes (V_A for the I_A element). In a similar manner, the tripping times for phases B and C are computed using the corresponding phase currents and voltages (i.e., V_B for the I_B element, and V_C for the I_C element).

In traditional relays, the element with the greatest current magnitude operates since the relay characteristic is dependent on the fault current magnitude only. This will not necessarily be the same for the proposed characteristic since it depends on voltage and current. The voltage magnitude K setting, and current magnitude will all simultaneously decide on the fastest operating element. For any fault type, the algorithm will measure the magnitude of each phase voltage and current. The operating time for each pair of phase quantities (V_A and I_A, V_B and I_B, V_C and I_C) is calculated using (1), and the fastest element will determine the overall operating time of the relay. This applies to primary and backup relays. Thus, the results reported in this paper present the fastest operating element.

III. Protection Coordination Problem Formulation

The protection coordination problem is developed for each system in order to find the optimal settings of each DOCR for three cases considered in this study. Case 1 is basically formulating and solving the problem using DOCRs with a conventional standard inverse time–current characteristic, while cases 2 and 3 use DOCRs equipped with the proposed time–current–voltage characteristic. Case 2 is solved considering that all DOCRs will have the same value for K while in case 3, the optimization is designed such that each DOCR can have a different value for the K setting. In each case, all relays were assumed to be identical where they are equipped with the same tripping characteristic.

The main objective of the protection coordination optimization (PCO) model is to minimize the sum of DOCRs operating time (T) (including the operating times of DOCRs due to SLG, LL, DLG, and three phase faults occurring at near end, mid, and far end on each line of a system) subject to protection coordination, relay setting, and relay operating time constraints. Therefore, the objective function can be represented as follows:

$$\text{Minimize } T = \sum_{i=1}^{N}\sum_{j=1}^{M}\sum_{l=1}^{L}\left(t_{ijl}^{p} + \sum_{x=1}^{X} t_{ijl}^{b_{xijl}}\right) \tag{2}$$

where N is the total number of relays with i being the relay identifier, M is the total number of fault types studied with j being the fault type identifier, and L is the total number of fault locations investigated with l being the fault-location identifier. The superscript p represents primary relays, while bx represents the backup relay x with X being the total number of backup relays for each primary relay. The backup relay x is dependent on the primary relay i for a fault type j that occurred at location l. The variables t_{ijl}^{p} and $t_{ijl}^{b_{xijl}}$ refer to the primary and backup relay i operating time for a fault of type j at location l, respectively.

The main optimization decision variables are the relay settings which depend on the case considered. The pickup current settings Ip are predetermined based on the values given in [31] and [32]. Thus, these values are considered as given parameters in the PCO model. On the other hand, TDS_i for N DOCRs are the variables of the PCO model in case 1. For case 2, the variables are TDS_i and one additional variable K. As for case 3, the variables are TDS_i, and K_i for N DOCRs. Therefore, case 1 is an LP problem since the conventional characteristic is linearized (fixed Ip settings). However, cases 2 and 3 are an NLP problem due to the nonlinearity of the proposed DOCR tripping characteristic. Yet, both types of formulations have the same objective function and set of constraints.

The PCO model involves satisfying the protection coordination constraints. Each primary DOCR in a system requires a backup DOCR to operate in the event of failing to isolate the fault in its zone. Thus, the coordination time interval (CTI) is the minimum gap in time between the operation of the primary and backup DOCRs that must be maintained. In this paper, CTI

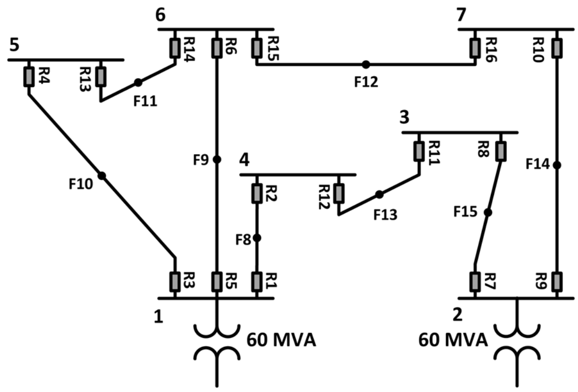

Fig. 3. Power distribution system of the IEEE 14-bus system under study.

is considered to be 0.3 s. This constraint can be expressed as follows:

$$t_{jl}^{b_x} - t_{jl}^{p} \geqslant \mathrm{CTI}\ \forall j,\ \{l, x\}. \tag{3}$$

Additional constraints are imposed on TDS settings and relay operating time. These constraints can be expressed as

$$\mathrm{TDS}_{i-min} \leqslant \mathrm{TDS}_i \leqslant \mathrm{TDS}_{i-max}\ \forall i \tag{4}$$

$$t_{ijl}^{p}, t_{ijl}^{b_x} \geqslant t_{ijl-min}\ \forall i, j, \{l, x\}. \tag{5}$$

The lower and upper limits on the DOCR's TDS ($\mathrm{TDS_{i-min}}$ and $\mathrm{TDS_{i-max}}$) are set to 0.05 and 1, respectively. Finally, the operating time of each primary and backup DOCR for all fault types and locations is constrained by a lower limit set to 20 ms [30].

IV. System Details and Simulation Setup

This section describes the test systems under study. The main study consists of a total of 16 possible system scenarios that are generated based on IEEE 14-bus and IEEE 30-bus standard distribution networks by varying the DG location. The single-line diagram of the IEEE 14-bus test system is shown in Fig. 3 [33]. This meshed distribution network is fed through two 60-MVA 132-kV/33-kV utility transformers with 10% transient reactance connected at buses 1 and 2. The system is equipped with 16 DOCRs. Fig. 3 shows nodes (F8–F15) where each one represents a set of faults on each line. For instance, F8 consists of a set of bolted SLG, LL, DLG, and three-phase faults occurring at near-end, midpoint, and far-end locations that are investigated on the line between buses 1 and 4.

Based on this system, six scenarios were created where the first is the base scenario with no DG units installed, and the remaining five scenarios are developed by adding DG units to the system each time. As shown in Table I, the DG units utilized in this study are each rated at 2MVA, synchronous type with 9.67% transient reactance, and are connected to the system through a 480-V/33-kV stepup transformer with 5% transient reactance. Each fault is associated with two primary DOCRs, one from each side that are each backed up by other DOCRs. For example, if a bolted three phase near-end (close to R1) fault occurs at node $F8_{n-3p}$, R1 and R2 are the two primary DOCRs. R1 is backed up by R4 and R6 while R2 is backed up by R11. Thus, for each fault location, primary and backup DOCRs are defined and accordingly implemented in the PCO models.

TABLE I
Description of System Scenarios

Scenario	Number of DG(s) / Type of system	Connection Bus(es)
1	0 / 14-bus	N/A
2	1 / 14-bus	3
3	2 / 14-bus	3,4
4	3 / 14-bus	3,4,5
5	4 / 14-bus	3,4,5,6
6	5 / 14-bus	3,4,5,6,7
7	0 / 30-bus	N/A
8	1 / 30-bus	3
90	2 / 30-bus	3,4
10	3 / 30-bus	3,4,5
11	4 / 30-bus	3,4,5,7
12	5 / 30-bus	3,4,5,7,10
13	6 / 30-bus	3,4,5,7,10,11
14	7 / 30-bus	3,4,5,7,10,11,13
15	8 / 30-bus	3,4,5,7,10,11,13,14
16	9 / 30-bus	1,3,4,5,7,10,11,13,14

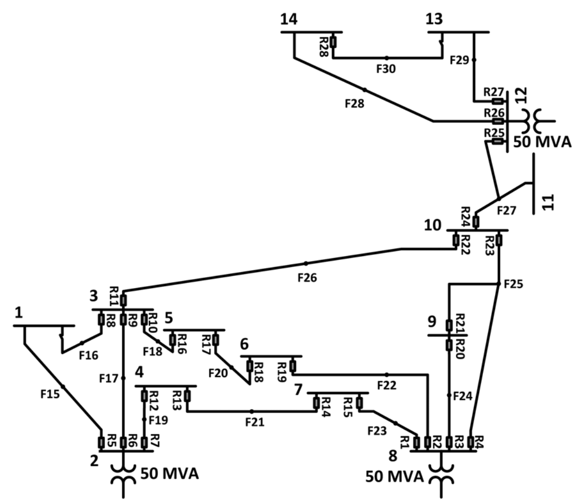

Fig. 4. Power distribution system of the IEEE 30-bus system under study.

Similarly, an additional nine system scenarios are generated based on the IEEE 30-bus distribution network [33]. The standard single-line diagram of the system is shown in Fig. 4. The base selected for all the systems under study is 100 MVA and 33 kV. A summary of the system scenarios investigated is given in Table I.

The optimization model developed for each system scenario for cases 2 and 3 is solved by using the MATLAB minimum-constrained nonlinear multivariable function [34]. This built-in MATLAB function relies on the reduced gradient approach (first-order optimality) for solving constrained nonlinear optimization problems. There are several algorithms available for solving a constrained nonlinear programming problem. The sequential quadratic programming (SQP) algorithm is chosen to solve the PCO models [18], [35]. A full description of the MATLAB SQP algorithm is provided in [34]. On the other hand, the PCO model that has been developed for each scenario, for case 1, is solved using the Simplex technique.

This article has been accepted for inclusion in a future issue of this journal. Content is final as presented, with the exception of pagination.

TABLE II
OPTIMAL TDS, Ip AND K CONSIDERING CASES 1–3

Relay	All Cases $Ip(A)$	Case 1 $TDS(s)$	Case 2 $TDS(s)$	Case 2 K	Case 3 $TDS(s)$	Case 3 K
1	300	0.515	0.562	1.15	0.619	1.81
2	300	0.309	0.411	1.15	0.349	1.2
3	200	0.396	0.477	1.15	0.461	1.29
4	60	0.6	1	1.15	1	1.35
5	700	0.295	0.368	1.15	0.473	1.92
6	140	0.442	0.6	1.15	0.803	1.79
7	900	0.29	0.374	1.15	0.406	1.51
8	300	0.366	0.484	1.15	0.321	1.15
9	400	0.432	0.438	1.15	0.585	2.44
10	250	0.316	0.42	1.15	0.376	1.21
11	400	0.343	0.417	1.15	0.651	1.99
12	600	0.282	0.352	1.15	0.355	1.48
13	250	0.265	0.385	1.15	0.32	1.16
14	300	0.4	0.53	1.15	1	2.36
15	400	0.304	0.337	1.15	0.332	1.42
16	100	0.61	0.766	1.15	1	1.89
$T(s)$		886.01	634.13		542.75	

V. OPTIMAL RELAY SETTINGS USING THE PROPOSED TIME–CURRENT–VOLTAGE CHARACTERISTIC

The protection coordination problem presented in Section III is solved by considering the conventional DOCR time–current characteristic and the proposed DOCR time–current–voltage characteristic. The optimal DOCR settings as well as operating times are determined for all of the presented 16 system scenarios. Comprehensive analysis of the results obtained for all of the investigated system scenarios is presented.

A. Simulation Results of the IEEE 14-bus System With 5 DGs

In this subsection, the simulation results obtained for system scenario 6 (refer to Table I), which consists of five synchronous-based DG units connected at buses 3– 7 on the IEEE 14-bus power distribution network, are analyzed. The optimal values of TDS_i and K_i as well as the objective function values T considering the conventional characteristic (case 1) and the proposed relay characteristic (cases 2 and 3) are presented in Table II.

As can be seen from the results, the relay Ip setting is fixed for all cases while the TDS values have changed when considering the proposed characteristic. The optimal DOCR settings achieved in each case ensure proper coordination of the DOCRs under SLG, DLG, LL, or three-phase faults that can occur at the near-end, mid, or far-end location on each line of the system. Moreover, the total relay operating time T is reduced by 28.4% in case 2 (considering the same K setting for all relays) with respect to case 1 (conventional characteristic). Further reduction in T (38.7% compared to case 1) is achieved in case 3 where the optimal value of K is determined for each DOCR. As can be seen, the new proposed time–current–voltage characteristic is capable of achieving better overall relay operating time compared to the conventional time–current characteristic. For brevity, a breakdown of the DOCR operation times due to three-phase, LL, DLG, and SLG faults at the midpoint on each line are given in Tables III–VI considering the conventional case and the case where K can vary for each relay (case 3), respectively. The operating time of each primary and backup DOCR satisfies the relay operating time constraint. It is also observed that all primary-backup relays are correctly coordinated with a minimum value of 300 ms for CTI. Also, it can be seen that for all fault types, the relay tripping times obtained from the proposed relay characteristic are always faster than the times attained from the conventional relay characteristic. Similar observations have been noticed for other scenarios.

TABLE III
OPTIMAL PRIMARY AND BACKUP RELAY OPERATING TIMES OF SCENARIO 6 - CASE 1/CASE 3 DUE TO THREE-PHASE FAULTS

Fault location	Operating times of relays (s) (p=primary, b=backup) Conventional Characteristic p	Conventional $b1$	Conventional $b2$	Proposed Characteristic p	Proposed $b1$	Proposed $b2$
F8	***R1:*** 1.31	***R4:*** 3.01	***R6:*** 2.05	***R1:*** 0.43	***R4:*** 1.99	***R6:*** 1.12
	R2: 1.03	***R11:*** 1.40	-	***R2:*** 0.42	***R11:*** 0.82	-
F9	***R5:*** 1.04	***R2:*** 1.44	***R4:*** 2.67	***R5:*** 0.36	***R2:*** 0.76	***R4:*** 1.44
	R6: 1.14	***R13:*** 2.86	***R16:*** 1.63	***R6:*** 0.40	***R13:*** 1.31	***R16:*** 0.81
F10	***R3:*** 0.88	***R2:*** 1.57	***R6:*** 6.83	***R3:*** 0.44	***R2:*** 0.96	***R6:*** 3.74
	R4: 1.28	***R14:*** 1.92	-	***R4:*** 0.65	***R14:*** 0.98	-
F11	***R13:*** 0.88	***R3:*** 1.25	-	***R13:*** 0.41	***R3:*** 0.71	-
	R14: 1.14	***R5:*** 1.94	***R16:*** 1.73	***R14:*** 0.52	***R5:*** 1.06	***R16:*** 1.14
F12	***R15:*** 1.04	***R5:*** 1.77	***R13:*** 1.97	***R15:*** 0.44	***R5:*** 1.12	***R13:*** 1.24
	R16: 1.34	***R9:*** 1.85	-	***R16:*** 0.52	***R9:*** 0.90	-
F13	***R11:*** 1.08	***R7:*** 1.53	-	***R11:*** 0.43	***R7:*** 0.84	-
	R12: 1.27	***R1:*** 1.64	-	***R12:*** 0.47	***R1:*** 0.78	-
F14	***R9:*** 1.27	***R8:*** 2.14	-	***R9:*** 0.35	***R8:*** 0.95	-
	R10: 1.11	***R15:*** 1.54	-	***R10:*** 0.47	***R15:*** 0.82	-
F15	***R7:*** 1.14	***R10:*** 1.60	-	***R7:*** 0.43	***R10:*** 0.82	-
	R8: 1.26	***R12:*** 1.63	-	***R8:*** 0.37	***R12:*** 0.72	-

TABLE IV
OPTIMAL PRIMARY AND BACKUP RELAY OPERATING TIMES OF SCENARIO 6 - CASE 1/CASE 3 DUE TO LL FAULTS

Fault location	Operating times of relays (s) (p=primary, b=backup) Conventional Characteristic p	Conventional $b1$	Conventional $b2$	Proposed Characteristic p	Proposed $b1$	Proposed $b2$
F8	***R1:*** 1.39	***R4:*** 3.36	***R6:*** 2.27	***R1:*** 0.82	***R4:*** 3.35	***R6:*** 2.14
	R2: 1.10	***R11:*** 1.53	-	***R2:*** 0.72	***R11:*** 1.49	-
F9	***R5:*** 1.13	***R2:*** 1.59	***R4:*** 2.95	***R5:*** 0.80	***R2:*** 1.19	***R4:*** 2.74
	R6: 1.20	***R13:*** 3.69	***R16:*** 1.73	***R6:*** 0.93	***R13:*** 2.70	***R16:*** 1.44
F10	***R3:*** 0.93	***R2:*** 1.75	***R6:*** 10.05	***R3:*** 0.68	***R2:*** 1.41	***R6:*** 9.58
	R4: 1.34	***R14:*** 2.14	-	***R4:*** 1.16	***R14:*** 2.10	-
F11	***R13:*** 0.95	***R3:*** 1.34	-	***R13:*** 0.72	***R3:*** 1.08	-
	R14: 1.22	***R5:*** 2.25	***R16:*** 1.84	***R14:*** 1.21	***R5:*** 2.08	***R16:*** 1.82
F12	***R15:*** 1.12	***R5:*** 2.03	***R13:*** 2.33	***R15:*** 0.71	***R5:*** 1.94	***R13:*** 1.98
	R16: 1.41	***R9:*** 2.04	-	***R16:*** 1.04	***R9:*** 1.56	-
F13	***R11:*** 1.16	***R7:*** 1.72	-	***R11:*** 0.93	***R7:*** 1.41	-
	R12: 1.40	***R1:*** 1.76	-	***R12:*** 0.90	***R1:*** 1.26	-
F14	***R9:*** 1.35	***R8:*** 2.44	-	***R9:*** 0.76	***R8:*** 1.46	-
	R10: 1.20	***R15:*** 1.72	-	***R10:*** 0.82	***R15:*** 1.25	-
F15	***R7:*** 1.25	***R10:*** 1.79	-	***R7:*** 0.87	***R10:*** 1.33	-
	R8: 1.36	***R12:*** 1.86	-	***R8:*** 0.68	***R12:*** 1.29	-

B. Comprehensive Analysis

In order to test the performance of the proposed DOCR characteristic, the problem formulation presented in Section III is applied to the 16 scenarios given in Table I with each relay equipped with the proposed time–current–voltage characteristic. The overall minimum operating time T for the three cases that are implemented on the 16 system scenarios is summarized in Table VII. In general, it can be seen that the proposed time–current–voltage characteristic (both cases 2 and 3) achieves a better overall minimum operating time in all scenarios. For the cases where no DG units are present in the system (system scenario 1 for the IEEE 14-bus system and 7 for the IEEE 30-bus system), in comparison to case 1, a reduction in T of 23.2% and 11% was achieved in case 2 while 33% and 21.5% were achieved in case 3, respectively. Thus, the proposed relay characteristic outperforms the conventional characteristic in cases where no DG is present. In addition,

This article has been accepted for inclusion in a future issue of this journal. Content is final as presented, with the exception of pagination.

TABLE V
OPTIMAL PRIMARY AND BACKUP RELAY OPERATING TIMES OF SCENARIO 6 - CASE 1/CASE 3 DUE TO DLG FAULTS

Fault location	Operating times of relays (s) (p=primary, b=backup)					
	Conventional Characteristic			Proposed Characteristic		
	p	$b1$	$b2$	p	$b1$	$b2$
F8	***R1:*** 1.33	***R4:*** 3.16	***R6:*** 2.15	***R1:*** 0.49	***R4:*** 2.31	***R6:*** 1.34
	R2: 1.06	***R11:*** 1.45	-	***R2:*** 0.44	***R11:*** 0.96	-
F9	***R5:*** 1.06	***R2:*** 1.51	***R4:*** 2.72	***R5:*** 0.41	***R2:*** 0.87	***R4:*** 1.55
	R6: 1.16	***R13:*** 2.98	***R16:*** 1.67	***R6:*** 0.42	***R13:*** 1.43	***R16:*** 0.92
F10	***R3:*** 0.90	***R2:*** 1.66	***R6:*** 8.48	***R3:*** 0.49	***R2:*** 1.11	***R6:*** 5.14
	R4: 1.30	***R14:*** 2.01	-	***R4:*** 0.68	***R14:*** 1.18	-
F11	***R13:*** 0.91	***R3:*** 1.28	-	***R13:*** 0.43	***R3:*** 0.80	-
	R14: 1.17	***R5:*** 2.03	***R16:*** 1.78	***R14:*** 0.60	***R5:*** 1.30	***R16:*** 1.32
F12	***R15:*** 1.07	***R5:*** 1.88	***R13:*** 2.12	***R15:*** 0.49	***R5:*** 1.38	***R13:*** 1.44
	R16: 1.38	***R9:*** 1.94	-	***R16:*** 0.57	***R9:*** 1.14	-
F13	***R11:*** 1.11	***R7:*** 1.60	-	***R11:*** 0.48	***R7:*** 0.98	-
	R12: 1.33	***R1:*** 1.69	-	***R12:*** 0.51	***R1:*** 0.93	-
F14	***R9:*** 1.30	***R8:*** 2.29	-	***R9:*** 0.43	***R8:*** 1.10	-
	R10: 1.15	***R15:*** 1.62	-	***R10:*** 0.50	***R15:*** 0.95	-
F15	***R7:*** 1.17	***R10:*** 1.68	-	***R7:*** 0.47	***R10:*** 0.92	-
	R8: 1.30	***R12:*** 1.72	-	***R8:*** 0.39	***R12:*** 0.81	-

TABLE VI
OPTIMAL PRIMARY AND BACKUP RELAY OPERATING TIMES OF SCENARIO 6 - CASE 1/CASE 3 DUE TO SLG FAULTS

Fault location	Operating times of relays (s) (p=primary, b=backup)					
	Conventional Characteristic			Proposed Characteristic		
	p	$b1$	$b2$	p	$b1$	$b2$
F8	***R1:*** 1.41	***R4:*** 3.70	***R6:*** 2.56	***R1:*** 0.56	***R4:*** 2.88	***R6:*** 1.73
	R2: 1.16	***R11:*** 1.65	-	***R2:*** 0.50	***R11:*** 1.18	-
F9	***R5:*** 1.13	***R2:*** 1.80	***R4:*** 2.96	***R5:*** 0.47	***R2:*** 1.09	***R4:*** 1.75
	R6: 1.23	***R13:*** 3.53	***R16:*** 1.81	***R6:*** 0.46	***R13:*** 1.76	***R16:*** 1.06
F10	***R3:*** 0.96	***R2:*** 2.15	***R6:*** 7.87	***R3:*** 0.55	***R2:*** 1.51	***R6:*** 5.10
	R4: 1.38	***R14:*** 2.35	-	***R4:*** 0.74	***R14:*** 1.50	-
F11	***R13:*** 1.01	***R3:*** 1.43	-	***R13:*** 0.49	***R3:*** 0.95	-
	R14: 1.29	***R5:*** 2.56	***R16:*** 2.02	***R14:*** 0.70	***R5:*** 1.77	***R16:*** 1.59
F12	***R15:*** 1.21	***R5:*** 2.41	***R13:*** 2.87	***R15:*** 0.58	***R5:*** 1.94	***R13:*** 2.06
	R16: 1.49	***R9:*** 2.31	-	***R16:*** 0.65	***R9:*** 1.52	-
F13	***R11:*** 1.21	***R7:*** 1.86	-	***R11:*** 0.55	***R7:*** 1.24	-
	R12: 1.52	***R1:*** 1.688	-	***R12:*** 0.60	***R1:*** 1.13	-
F14	***R9:*** 1.41	***R8:*** 3.06	-	***R9:*** 0.52	***R8:*** 1.56	-
	R10: 1.29	***R15:*** 1.96	-	***R10:*** 0.58	***R15:*** 1.22	-
F15	***R7:*** 1.23	***R10:*** 1.99	-	***R7:*** 0.51	***R10:*** 1.14	-
	R8: 1.41	***R12:*** 2.03	-	***R8:*** 0.43	***R12:*** 0.99	-

irrespective of the number of DG units, in the system size as well as DG location, the proposed relay characteristic can achieve significantly better DOCR operating time. For the IEEE 14-bus system, the percentage reduction in T varies from 21.3% to 33.6% in case 2 whereas it is 28.7% to 48% in case 3. On the other hand, percentage reductions in T range from 4.69% to 11.4% in case 2 while 20.7% to 27.6% in case 3 were obtained for the IEEE 30-bus system. The amount of reduction in T is dependent on the number of DGs as well as location.

Table VIII shows the optimal K value obtained in case 2 (considering the same K for all relays) when solving the PCO model for each system scenario. The optimal K value for the IEEE 14-bus system (system 1 up to 6) roughly varies around the value of 1 while for the IEEE 30-bus system, it is limited to a small value around zero. As can be seen, the K setting varies depending on the system scenario and can be optimally set using the proposed model. Small K values limit the fault voltage magnitude effect and, thus, limit the amount of reduction achieved with respect to case 1. Allowing each relay to have its own optimal K can achieve higher reduction in T. It is worth noting that setting a fixed value of K for all relays versus allowing the value of K to be different for each relay will depend on the protection engineer designer preference.

TABLE VII
TOTAL RELAYS OPERATING TIME FOR ALL CASES AND SCENARIOS

Total relays operating time $T(s)$							
Scenario	*Case 1*	*Case 2*	*Case 3*	*Scenario*	*Case 1*	*Case 2*	*Case 3*
1	827.9	635.4	554.7	9	10746	9540	8457
2	954.3	751.2	638.2	10	10263	9153	8079
3	844.4	649.1	561	11	9840	8716	7799
4	1042	803.9	742.8	12	13864	13214	10324
5	1589	1056	825.4	13	12161	11020	9026
6	886	634.1	542.8	14	12478	11321	9161
7	11511	10249	9033	15	12821	11657	9314
8	11759	10580	9199	16	12781	11652	9257

TABLE VIII
OPTIMAL K FOR CASE 2–ALL SCENARIOS

Scenario	K	*Scenario*	K
1	0.8854	9	0.0765
2	0.8828	10	0.0714
3	0.8764	11	0.0655
4	1.1315	12	0.0613
5	0.9046	13	0.0595
6	1.1528	14	0.0586
7	0.0805	15	0.0578
8	0.0791	16	0.0551

TABLE IX
PERCENTAGE REDUCTION IN TIME WITH RESPECT TO CASE 1 FOR DIFFERENT SYSTEM SCENARIOS

Type of DG units	Number of DGs	DGs locations	Reduction in T (%) *Case 2*	*Case 3*
Inverter	2	3,4	12.15	20.36
Synchronous	0	-		
Inverter	4	3,4,5,7	10.08	21.25
Synchronous	0	-		
Inverter	3	4,5,7	8.86	21.52
Synchronous	1	3		
Inverter	1	3	9.22	21.02
Synchronous	3	4,5,7		

C. Performance of the Proposed Characteristic in the Presence of the Inverter-Based DG

The impact of inverter-based and synchronous-based DG units on the amount of percentage reduction that can be achieved using the proposed characteristic is investigated in this subsection. Four system scenarios were implemented considering K to be fixed for all relays (case 2) and variable (case 3). Each system scenario has either inverter-based DG units or a combination of inverter-based and synchronous-based DG units connected to the IEEE 30-bus network. The synchronous-based DG units are rated at 2 MVA with the specifications mentioned previously. On the other hand, the inverter-based DG units are rated at 2 MVA and are controlled in the constant current mode. Thus, they are modeled as ideal current sources injecting 2 p.u. of the DG-rated capacity during fault conditions. Table IX shows the four system scenarios and the corresponding resulting percentage reduction in total relays operating time T with respect to case 1.

TABLE X
PRECENTAGE REDUCTION IN TIME WITH RESPECT TO CASE 1 FOR DIFFERENT DG CAPACITIES AND LOCATIONS

Type of System	DG location	DG Capacity (MVA)	Reduction in T (%) *Case 2*	*Case 3*
IEEE 14-Bus Network	3	2	21.28	33.12
		5	24.13	34.87
		9	24.69	34.7
	6	2	26.31	35.84
		5	23.44	39
		9	27.61	41.6
	7	2	25.01	34.5
		5	27.1	36.1
		9	27.32	38.71
IEEE 30-Bus Network	3	2	10.03	21.77
		5	7.08	22.27
		9	7.27	24
	4	2	12.04	20.89
		5	12.36	20.61
		9	11.43	20.38
	14	2	11.28	21.38
		5	9.68	22.03
		9	4.27	23.19

The resulting percentage reduction in T confirms that regardless of type of DG unit connected to a network, the proposed relay characteristic (case 2 and 3) will achieve significant improvement with respect to the conventional characteristic. Moreover, the amount of percentage reduction is affected by the type of DG installed.

D. Impact of DG Capacity and Location

Since the synchronous-based DG unit has a more profound impact on short-circuit current, this subsection analyzes the impact of the synchronous-based DG unit's capacity and location on the amount of percentage reduction that can be achieved using the proposed relay characteristic. Multiple simulations were performed considering K to be fixed for all relays (case2) and variable (case3). For each simulation, the DG is installed at a specific location while varying its capacity. For brevity, for each system, three locations are investigated for DG capacities of 2 MVA, 5 MVA, and 9 MVA. Table X demonstrates the 18 simulation setups and the corresponding resulting percentage reduction in total relays operating time T with respect to case 1.

From the results, three main observations can be deduced. First, case 3 achieves a higher percentage reduction in T with respect to case 1 than case 2 in all simulation setups. Second, it is clear that the amount of percentage reduction depends on the network (IEEE 14 bus or IEEE 30 bus) to which the new proposed DOCRs are connected. Finally, it is observed that depending on the location and capacity of DG in the network, the amount of percentage reduction experiences slight variation in cases 2 and 3. Although there is no general trend to the amount of reduction with respect to an increase in DG capacity at a given location, the proposed relay characteristic always outperforms the conventional time–current characteristic and, thus, can reduce the overall relay's operating time for all cases.

It is worth noting that the analysis performed in this paper is based on a fixed network topology. Power systems may experience changes in the network topology due to various reasons, such as network reconfigurations, maintenance activities, and isolation of faulted sections [8]. In such occasions, some of the primary/backup DOCR pairs for specific faults may not be coordinated correctly. According to [8], [9], [13], and [31], proper coordination can be achieved by modifying the PCO model to include additional sets of coordination constraints that consider all network topologies due to single-line outage contingencies in a system. This will result in optimal DOCR settings that are different from the optimal DOCR settings achieved under the assumption of fixed network topology. In addition to the above concern, the fault current direction might change with changes in the network topology. This issue was not addressed in previous work focusing on protection coordination. In this paper, the effect of dynamic changes in the network topology has not been considered.

VI. CONCLUSION

This paper proposes a new time–current–voltage relay characteristic that can be utilized by DOCRs in a meshed distribution network in the presence of DG units. The proposed characteristic relies on utilizing the fault voltage magnitude in addition to the current to determine the operating time of DOCRs. In addition to the commonly used relays settings, a third relay setting K, responsible for tuning the effect of voltage on relay operating time, was introduced. This setting can either have a fixed common value for all DOCRs or each DOCR can have its own optimal K setting value. The protection coordination problem is formulated and solved considering the conventional and proposed relay characteristic. The optimal settings attained by solving the PCO model for cases with either a conventional or proposed DOCR characteristic ensure proper coordination of all DCORs under SLG, DLG, LL, and three-phase faults that might occur at near-end, mid, and far-end locations on each line of a system. The results show that the utilization of the proposed time–current–voltage characteristic for each DOCR in a meshed distribution network can achieve a significant reduction in the total relay operating time T in the absence and presence of synchronous-based and inverter-based DG. The amount of reduction will depend on the system structure, type, number, and capacity as well as the location of DG units. In addition, by setting each relay with its optimal K settings (as opposed to having the same value of K for all relays), further reduction in the overall relays' operating time can be achieved.

REFERENCES

[1] P. Sutherland, "Protective device coordination in an industrial power system with multiple sources," *IEEE Trans. Ind. Appl.*, vol. 33, no. 4, pp. 1096–1103, Jul. 1997.

[2] J.-H. Teng, "Unsymmetrical short-circuit fault analysis for weakly meshed distribution systems," *IEEE Trans. Power Syst.*, vol. 25, no. 1, pp. 96–105, Feb. 2010.

[3] B. Hussain, S. Sharkh, and S. Hussain, "Impact studies of distributed generation on power quality and protection setup of an existing distribution network," in *Proc. IEEE Int. Symp. Power Electron. Elect. Drives Autom. Motion*, 2010, pp. 1243–1246.

[4] W. El-khattam and T. Sidhu, "Restoration of directional overcurrent relay coordination in distributed generation systems utilizing fault current limiter," *IEEE Trans. Power Del.*, vol. 23, no. 2, pp. 576–585, Apr. 2008.

[5] W. Najy, H. Zeineldin, and W. Woon, "Optimal protection coordination for microgrids with grid-connected and islanded capability," *IEEE Trans. Ind. Electron.*, vol. 60, no. 4, pp. 1668–1677, Apr. 2013.

[6] V. Pandi, H. Zeineldin, and W. Xiao, "Determining optimal location and size of distributed generation resources considering harmonic and protection coordination limits," *IEEE Trans. Power Syst.*, vol. 28, no. 2, pp. 1245–1254, May 2013.
[7] H. Zeineldin, Y.-R. Mohamed, V. Khadkikar, and V. Pandi, "A protection coordination index for evaluating distributed generation impacts on protection for meshed distribution systems," *IEEE Trans. Smart Grid*, vol. 4, no. 3, pp. 1523–1532, Sep. 2013.
[8] A. S. Noghabi, J. Sadeh, and H. R. Mashhadi, "Considering different network topologies in optimal overcurrent relay coordination using a hybrid ga," *IEEE Trans. Power Del.*, vol. 24, no. 4, pp. 1857–1863, Oct. 2009.
[9] A. Urdaneta, R. Nadira, and L. Perez Jimenez, "Optimal coordination of directional overcurrent relays in interconnected power systems," *IEEE Trans. Power Del.*, vol. 3, no. 3, pp. 903–911, Jul. 1988.
[10] A. Urdaneta, H. Restrepo, S. Marquez, and J. Sanchez, "Coordination of directional overcurrent relay timing using linear programming," *IEEE Trans. Power Del.*, vol. 11, no. 1, pp. 122–129, Jan. 1996.
[11] A. Urdaneta, L. Perez, J. Gomez, B. Feijoo, and M. Gonzalez, "Presolve analysis and interior point solutions of the linear programming coordination problem of directional overcurrent relays," *Int. J. Elect. Power Energy Syst.*, vol. 23, no. 8, pp. 819–825, 2001.
[12] B. Chattopadhyay, M. Sachdev, and T. Sidhu, "An on-line relay coordination algorithm for adaptive protection using linear programming technique," *IEEE Trans. Power Del.*, vol. 11, no. 1, pp. 165–173, Jan. 1996.
[13] A. Urdaneta, L. Perez, and H. Restrepo, "Optimal coordination of directional overcurrent relays considering dynamic changes in the network topology," *IEEE Trans. Power Del.*, vol. 12, no. 4, pp. 1458–1464, Oct. 1997.
[14] C. W. So and K. K. Li, "Time coordination method for power system protection by evolutionary algorithm," *IEEE Trans. Ind. Appl.*, vol. 36, no. 5, pp. 1235–1240, Sep. 2000.
[15] P. Bedekar, S. Bhide, and V. Kale, "Optimum coordination of overcurrent relays in distribution system using genetic algorithm," in *Proc. Int. Conf. Power Syst.*, Dec. 2009, pp. 1–6.
[16] M. M. Mansour, S. F. Mekhamer, and N. EL-SHERIF EL-KHARBAWE, "A modified particle swarm optimizer for the coordination of directional overcurrent relays," *IEEE Trans. Power Del.*, vol. 22, no. 3, pp. 1400–1410, Jul. 2007.
[17] H. Zeineldin, E. El-Saadany, and M. Salama, "Optimal coordination of overcurrent relays using a modified particle swarm optimization," *Elect. Power Syst. Res.*, vol. 76, no. 11, pp. 988–995, 2006.
[18] D. Birla, R. Maheshwari, and H. Gupta, "A new nonlinear directional overcurrent relay coordination technique, banes and boons of near-end faults based approach," *IEEE Trans. Power Del.*, vol. 21, no. 3, pp. 1176–1182, Jul. 2006.
[19] T. Keil and J. Jager, "Advanced coordination method for overcurrent protection relays using nonstandard tripping characteristics," *IEEE Trans. Power Del.*, vol. 23, no. 1, pp. 52–57, Jan. 2008.
[20] N. Nimpitiwan, G. Heydt, R. Ayyanar, and S. Suryanarayanan, "Fault current contribution from synchronous machine and inverter based distributed generators," *IEEE Trans. Power Del.*, vol. 22, no. 1, pp. 634–641, Jan. 2007.
[21] C. R. Mason, *The Art and Science of Protective Relaying*. Hoboken, NJ, USA: Wiley, 2012.
[22] *Single Input Energizing Quality Measuring Relays With Dependent or Independent*, IEC Publ. 255-3 (1989-05), 1989.
[23] T. Areva, *Network Protection & Automation Guide*. Barcelona, Spain: Cayfosa, 2002, pp. 92–95, layout by Flash Espace, Montpellier, France.
[24] *"Siprotec Multi-function Protective Relay With Local Control 7sj62/63/64 v4. 6 Manual,"* ver. Order No. C53000-G1140-C147-7, Siemens AG.
[25] J. Horak, "Directional overcurrent relaying (67) concepts," in *Proc. IEEE 59th Annu. Protect. Relay Eng. Conf.*, 2006, p. 13.
[26] A. Bakar, H. Mokhlis, H. Illias, and P. Chong, "The study of directional overcurrent relay and directional earth-fault protection application for 33 kv underground cable system in Malaysia," *Int. J. Elect. Power Energy Syst.*, vol. 40, no. 1, pp. 113–119, 2012.
[27] K. Zimmerman and D. Costello, "Fundamentals and improvements for directional relays," in *Proc. IEEE 63rd Annu. Conf. Protect. Relay Eng.*, 2010, pp. 1–12.
[28] *"Instruction Manual, Directional Overcurrent Protection Relay—GRD140,"* Toshiba, 2004.
[29] *"Directional/non Directional Overcurrent Protection. Technical Data Sheet (P12xy/EN TDS/H76),"* AREVA, 2012.
[30] J. L. Blackburn and T. J. Domin, *Protective Relaying: Principles and Applications*, 3rd ed. Boca Raton, FL, USA: CRC, 2007.
[31] A. S. Noghabi, H. R. Mashhadi, and J. Sadeh, "Optimal coordination of directional overcurrent relays considering different network topologies using interval linear programming," *IEEE Trans. Power Del.*, vol. 25, no. 3, pp. 1348–1354, Jul. 2010.
[32] M. Ezzeddine, R. Kaczmarek, and M. Iftikhar, "Coordination of directional overcurrent relays using a novel method to select their settings," *IET Gen., Transm. Distrib.*, vol. 5, no. 7, pp. 743–750, 2011.
[33] Univ. Washington, Seattle, WA, USA, "Power systems test case archive," Tech Rep., 2006. [Online]. Available: http://www.ee.washington.edu/research/pstca
[34] M. O. Toolbox, *Optimization Toolbox*. Natick, MA, USA: The Mathworks Inc., 2002.
[35] P. P. Bedekar and S. R. Bhide, "Optimum coordination of directional overcurrent relays using the hybrid ga-nlp approach," *IEEE Trans. Power Del.*, vol. 26, no. 1, pp. 109–119, Jan. 2011.

Khaled A. Saleh (S'12) was born in Cairo, Egypt, in 1991. He received the B.Sc. degree in electrical engineering from The Petroleum Institute, Abu Dhabi, United Arab Emirates (UAE), in 2012, the M.Sc. degree in electrical power engineering from Masdar Institute of Science and Technology, Abu Dhabi, UAE, in 2014, and is currently pursuing the Ph.D. degree in electrical and computer engineering from University of Waterloo, Waterloo, ON, Canada.

His current research interests include power system protection, distributed generation, system reconfiguration, and optimization techniques.

H. H. Zeineldin (M'06–SM'13) received the B.Sc. and M.Sc. degrees in electrical engineering from Cairo University, Cairo, Egypt, in 1999 and 2002, respectively, and the Ph.D. degree in electrical and computer engineering from the University of Waterloo, Waterloo, ON, Canada, in 2006.

He was with Smith and Andersen Electrical Engineering, Inc., where he was involved with projects involving distribution system design, protection, and distributed generation. He was then a Visiting Professor at the Massachusetts Institute of Technology, Cambridge, MA, USA. He is with the Faculty of Engineering, Cairo University, and currently he is an Associate Professor with the Masdar Institute of Science and Technology, Masdar City, UAE. He is currently an Editor of the IEEE TRANSACTIONS ON ENERGY CONVERSION and IEEE TRANSACTIONS ON SMART GRIDS. His current interests include power system protection, distributed generation, and deregulation.

A. Al-Hinai (M'08–SM'11) received the B.Sc. degree in electrical engineering from Sultan Qaboos University, Muscat, Oman, in 1997. He received the M.Sc. and Ph.D. degrees in electrical engineering from West Virginia University, Morgantown, WV, USA, in 2000 and 2005, respectively.

He joined Sultan Qaboos University as a Demonstrator in 1998. He is an Assistant Professor in the Electrical and Computer Engineering Department, Sultan Qaboos University. Currently, he is a Visiting Professor at Masdar Institute of Science and Technology, Abu Dhabi, United Arab Emirates. In addition, he is holding a member position at the Authority of Electricity Regulation, Oman. His areas of interest are power systems, such as control and operation, along with multiagent systems, applications for the control of power systems, optimization techniques, and applications for power systems.

Ehab F. El-Saadany (SM'05) was born in Cairo, Egypt, in 1964. He received the B.Sc. and M.Sc. degrees in electrical engineering from Ain Shams University, Cairo, Egypt, in 1986 and 1990, respectively, and the Ph.D. degree in electrical engineering from the University of Waterloo, Waterloo, ON, Canada, in 1998.

Currently, he is a Professor with the Department of Electrical and Computer Engineering, University of Waterloo. His current research interests include distribution system operation and control, distributed generation, smart-grid applications, self-healing mechanisms, power quality, and microelectromechanical-systems micropower generators.

Dr. El-Saadany is the holder of the Canada Research Chair in Smart Distribution Systems in recognition of his contributions to the areas of distributed generation and microgrids.